

Enhanced Diffraction Efficiency in a Photorefractive Liquid Crystal Cell with Poly(9-vinylcarbazole)-Infiltrated Mesoporous TiO₂ Layers

Kwang-Suk Jang,[†] Hyun-Wuk Kim,[‡] Sung-Ho Cho,[‡] and Jong-Duk Kim^{*,†}

Department of Chemical and Biomolecular Engineering (BK21 Graduate Program),
Korea Advanced Institute of Science and Technology, Daejeon 305-701, Republic of Korea, and
LCD Business, Samsung Electronics Co., Ltd., Yongin-City, Gyeonggi-Do 449-711, Republic of Korea

Received: June 25, 2006; In Final Form: September 21, 2006

The photorefractive effect of a layer-structured liquid crystal cell was significantly enhanced when a C₆₀-doped poly(9-vinylcarbazole) (PVK)/TiO₂ nanocomposite was used in two photoconductive layers. The C₆₀-doped PVK/TiO₂ nanocomposite film was prepared by infiltrating C₆₀-doped PVK into a highly ordered mesoporous TiO₂ layer. The addition of the TiO₂ layer to the C₆₀-doped PVK layer increased the first-order Raman–Nath diffraction efficiency from 24% to 42.9%. This enhancement of diffraction efficiency is attributed to a blocking effect of charge recombination in the composite layer. The electron transfer from the PVK layer into the TiO₂ layer would decrease the recombination of photogenerated charges in the PVK layer, while charges in the PVK layer could participate in the formation of a space-charge field.

1. Introduction

The photorefractive liquid crystal cell is widely considered to be a potentially useful device for signal and data processing and real-time holography.¹ Nematic liquid crystals (LCs) can be used for obtaining an orientational photorefractive effect because of their large Kerr-like optical nonlinearities associated with the orientation of the director axis. Furthermore, unlike electrooptically induced photorefractive polymers, they offer fast response to low voltage.² To date, several types of photorefractive liquid crystal (PR-LC) systems have been proposed, including pure LCs,³ charge generator doped LCs,⁴ monomer doped LCs,⁵ polymer dispersed LCs,⁶ and layer-structured LCs.⁷ Among them, the layer-structured PR-LC device exhibits the highest diffraction efficiency, because of efficient molecular reorientation of LCs between the photoconductive layers,⁷ where a spatially modulated charge field can be generated by spatially nonuniform light exposure. The space-charge field may force LCs to reorient and thus modulate the refractive index. In previously proposed layer-structured PR-LC systems, photosensitizer-doped PVK was used as a photoconductive layer.⁷ While PVK layers showed quite good performance for the photorefractive system, their photoconductivity was limited by low charge mobility and short exciton diffusion length.⁸ For enhancement of the photorefractive effect, charge separation and migration in a photoconductive layer must therefore be improved.

Here, we report a layer-structured PR-LC system with novel photoconductive layers composed of C₆₀-doped PVK/TiO₂ nanocomposite. The proposed system has a greatly enhanced photorefractive effect. Nanocrystalline TiO₂ is known to have excellent electron-transport ability, sufficient for use in a photovoltaic cell.⁹ Charge separation and transport through the TiO₂/polymer interface, intermixed on a nanometer length scale,

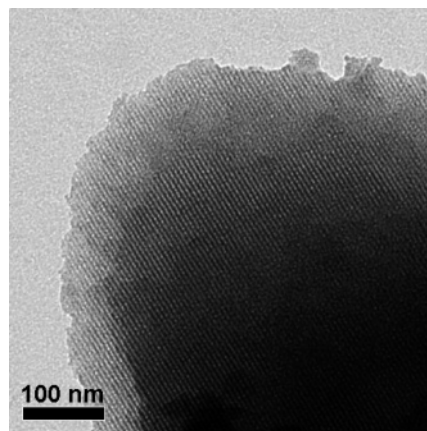


Figure 1. TEM image of the mesoporous TiO₂ thin film with uniformly close-packed cylindrical pores.

has been widely studied.¹⁰ Our approach is based on the above two aspects. Through electron injection into TiO₂ at the interface of the PVK/TiO₂ nanocomposite, charge recombination is reduced, and resultant increase in the number of holes in PVK could contribute to the space-charge field. This charge separation and transport mechanism were verified by the response behaviors of the first-order diffracted beam intensities.

2. Results and Discussion

The PVK/TiO₂ nanocomposite was synthesized with a highly ordered mesoporous TiO₂ film. The ordered structure of mesoporous materials was derived from supramolecular assemblies of surfactants or amphiphilic block copolymers within a range of 2–50 nm.¹¹ A thin film of mesoporous TiO₂ having a thickness of 160 nm was fabricated using polyoxyethylene-(20) cetyl ether as a structure-directing agent.¹² Figure 1 shows a TEM image of the mesoporous TiO₂ film. The TEM image shows the existence of uniformly close-packed cylindrical pores with a diameter of about 4 nm. In most TEM images, repeated straight lines of much greater than the film thickness could be

* Corresponding author. Telephone: +82-42-869-3961. Fax: +82-42-869-3910. E-mail: jdkim@kaist.ac.kr.

[†] Korea Advanced Institute of Science and Technology.

[‡] Samsung Electronics Co Ltd.

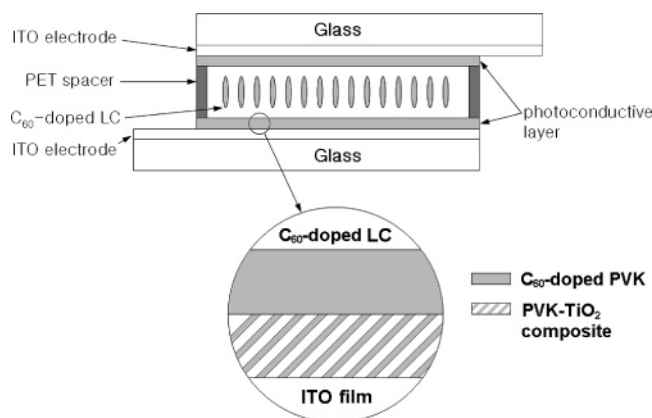


Figure 2. The structure of the fabricated PR-LC cell in a form of a LC layer sandwiched between two C_{60} -doped PVK/ TiO_2 nanocomposite layers.

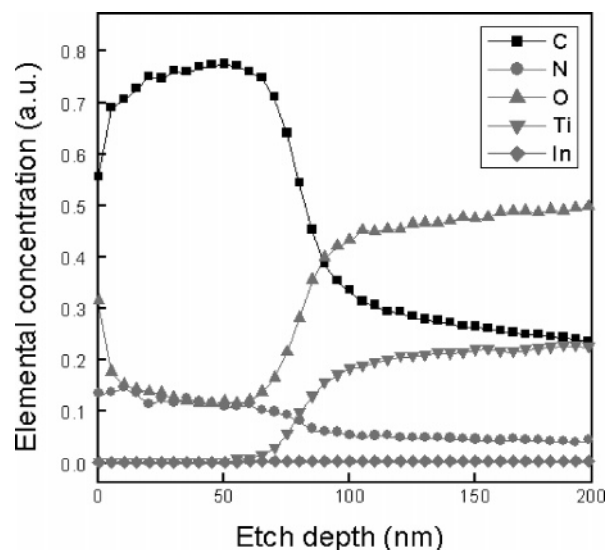


Figure 3. The XPS depth profiling of the C_{60} -doped PVK/ TiO_2 nanocomposite film whose polymer overlayer was rinsed with toluene.

observed. The pore structure could be indexed as a pseudo 2D centered-rectangular structure (c2m). The effect of contraction during calcination would modify the 2D hexagonal structure (p6m) of the template into the pseudo 2D centered-rectangular structure (c2m).¹² The detailed preparation method and structural characterization have been described in a previous work.¹²

PVK doped with 0.05 wt % C_{60} as a photosensitizer was deposited on the mesoporous TiO_2 layer by spin-coating. The double-layered film was heated to 240 °C for 7 h so as to infiltrate the polymer into mesoporous TiO_2 layer. After heat treatment, the polymer overlayer with a thickness of 200 nm remained, as shown in Figure 2. Heating of the polymer/mesoporous TiO_2 double-layered film above T_g allows the polymer chains to infiltrate down to the bottom of the mesoporous TiO_2 layers.¹³ This heat treatment method is similar to the fabrication method for polymer-layered silicate nanocomposite in which the thickness of the layered silicate gallery is even less than 1 nm.¹⁴

Figure 3 shows the XPS depth profile of the C_{60} -doped PVK/ TiO_2 nanocomposite film whose polymer overlayer was rinsed with toluene. The thickness of the polymer overlayer was reduced below 80 nm prior to the depth analysis, because the ion etching process has a depth limitation. Large amounts of carbon and nitrogen were detected in the mesoporous TiO_2 layer, while the mesoporous TiO_2 film without polymer infiltration

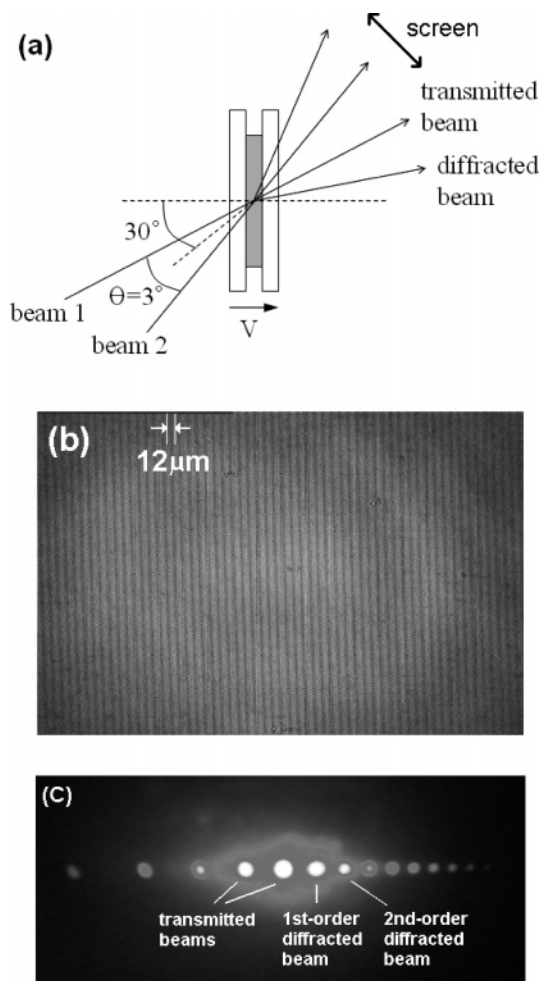


Figure 4. (a) Two-beam coupling experimental setup for the Raman–Nath diffraction. (b) The interference pattern of two p -polarized writing beams with the angle (θ) of 3°. (c) The Raman–Nath diffraction of the PR-LC cell with novel photoconductive layers.

contained carbon residue of less than 7% (see fig. S1). Therefore, it is believed that PVK should penetrate sufficiently into the mesoporous TiO_2 layer to form a well-defined C_{60} -doped PVK/ TiO_2 nanocomposite film.

Using this nanocomposite film as a photoconductive layer, layer-structured PR-LC cells were fabricated, as shown in Figure 2. The layer-structured PR-LC cell was fabricated in the form of a LC layer sandwiched between two C_{60} -doped PVK/ TiO_2 nanocomposite layers. The thickness of the LC layer, 9.5 μm , was determined by poly(ethylene terephthalate) (PET) spacers. And the C_{60} -doped nematic E7 (0.05:99.95 wt %) was injected at a nematic phase, because of a flow-induced orientation driven by capillary force, that is, molecular ordering at a flow field.^{15,16}

The diffraction efficiency of the fabricated PR-LC cell was determined by a general two-beam coupling experimental setup,¹⁷ as shown in Figure 4a. A He–Ne laser (the optical wavelength, $\lambda = 632.8 \text{ nm}$) with an intensity of 17 mW was used as a writing beam, and two p -polarized writing beams respectively had a peak intensity of 150 mW/cm². The angle (θ) between two writing beams is 3, which is measured in air, and the generated grating spacing, $\Lambda = \lambda/[2\sin(\theta/2)]$, is about 12 μm , as shown in Figure 4b. The cell tilt angle, the angle between the bisector of two writing beams and the direction normal to the cell surface, was 30. The Raman–Nath diffraction regime ($\Lambda^2 \gg d\lambda$)¹⁸ was satisfied, where d is the LC layer thickness. Many orders of diffraction appeared in the Raman–Nath diffraction regime where the angular spread of the grating

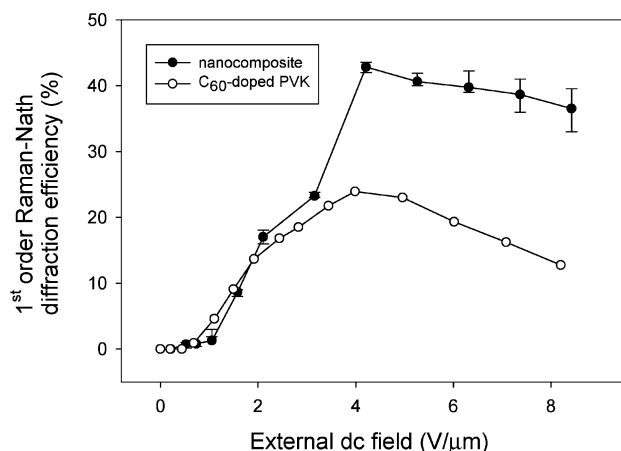


Figure 5. The first-order Raman–Nath diffraction efficiencies of the layer-structured PR-LC cells with C₆₀-doped PVK/TiO₂ nanocomposite layers (cell A, ●), and with C₆₀-doped PVK layers (cell B, ○) only.

wave vector is much larger than the Bragg angle. Figure 4c shows the Raman–Nath diffraction of the PR-LC cell with novel photoconductive layers. The diffraction efficiency is calculated as the first-order Raman–Nath diffraction efficiency, defined as follows:¹⁹

$$\eta(\%) = I_{\text{first-order diffracted beam}} / I_{\text{incident beam}} \times 100$$

which is the ratio of the intensity of a first-order diffracted beam to that of an incident beam.

For comparison, a reference PR-LC cell was fabricated with photoconductive layers of 0.05 wt % C₆₀-doped PVK.¹⁶ The PVK layer thickness in the reference cell is 200 nm, equivalent to the PVK overlayer thickness of the nanocomposite film. Figure 5 shows the first-order Raman–Nath diffraction efficiencies of the layer-structured PR-LC cells with C₆₀-doped PVK/TiO₂ nanocomposite layers (cell A, ●) and with C₆₀-doped PVK layers (cell B, ○) only. The LC layer thicknesses, 9.5 μm in the cell A and 7.5 μm in the cell B, were selected so as to yield maximum diffraction efficiencies, as determined in a previous work¹⁶ and shown in Figure S2. To ensure reliable results, the diffraction efficiency of cell A was measured three times with three cells and averaged. The maximum diffraction efficiency of cell B was 24%, similar to results reported elsewhere.¹⁶ However, the diffraction efficiency of cell A was greatly enhanced with a maximum diffraction efficiency of 42.9%, which is higher than the maximum possible diffraction efficiency (~34%) in the Raman–Nath theory of diffraction.²⁰ This result might be a direct consequence of a strongly nonsinusoidal form of spatial changes of refractive index in the volume of LC layer.²¹ It limits applicability of Raman–Nath diffraction theory developed for sinusoidal phase gratings.

The first-order Raman–Nath diffraction efficiency increased by about 20%, indicating that TiO₂ plays a significant role in a photoconduction. However, it is not clear how the space-charge field was enhanced in the novel photoconductive layer. One possible explanation of the field modulation is an electron transfer into the TiO₂ layer by charge separation at the PVK–TiO₂ interface.

In the previous system, such as that modeled in cell B, photosensitizers doped in PVK absorb photons and produce charges, and photogenerated holes are transported by a hopping process and trapped in local trapping sites. PVK acts as a hole transporter, and therefore a space-charge field is induced. Meanwhile, TiO₂ is an excellent electron transporter, such that it has been applied in a dye-sensitized solar cell.⁹ Therefore,

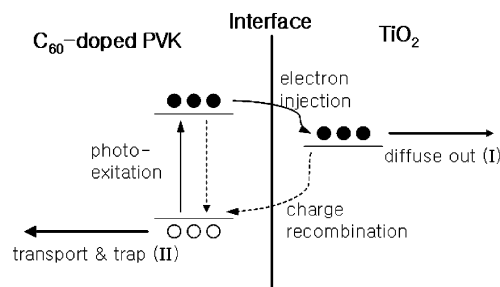


Figure 6. Schematic diagram of the spatial charge generation procedure at the interface of PVK and TiO₂.

PVK/TiO₂ nanocomposite could form a donor–acceptor heterojunction, leading to novel properties in a layer-structured PR-LC cell. The charge transport mechanism in polymer/TiO₂ composite has been widely studied for its photovoltaic use.¹⁰ Generally, charges are photogenerated in the polymer and dissociated at the polymer–TiO₂ interface. Such a charge separation process would act as a charge-recombination blocker that could interrupt charge recombination. Therefore, the area of interface between the polymer and TiO₂ is expected to play an important role in charge recombination. Notably the interface area should increase significantly when the composite is intermixed on a nanometer length scale.

Figure 6 shows a schematic diagram of the spatial charge generation procedure at the interface of PVK and TiO₂. In the photoconductive layer of the C₆₀-doped PVK/TiO₂ nanocomposite, it appears that the space-charge field forms as follows: charges are photogenerated in the C₆₀-doped PVK layer, and charge separation occurs at the TiO₂–PVK interface. Electrons are drained into the TiO₂ layer and diffuse out rapidly, and then holes are transported and trapped in the PVK layer. Finally, a space-charge field is induced by the trapped charges. Because PVK and TiO₂ have little absorbance in the visible range, the photosensitizer, C₆₀, was doped in PVK, and charges were photogenerated in the C₆₀-doped PVK layers. Although excitons in an organic solid can typically travel less than 20 nm before recombining,²² charge separation at the TiO₂–PVK heterojunction could occur because C₆₀-doped PVK and TiO₂ were intermixed on a nanometer length scale by infiltration of the polymer into the mesopores of TiO₂. As electrons were transported to the TiO₂ layer, recombination of photogenerated charges in the PVK layer would be reduced, and thus more charges could participate in the formation of the space-charge field.

To verify the role of the TiO₂ layer, i.e., to serve as an electron drain from the PVK layer, we fabricated another layer-structure PR-LC cell (cell C) whose photoconductive layers were cis-bis(isothiocyano)bis(2,2'-bipyridyl-4,4'-dicarboxyato)-ruthenium-(II) (N3)-chemisorbed mesoporous TiO₂.²³ Instead of the PVK infiltration process, described above, mesoporous TiO₂ film was immersed in a 0.5 mM N3/ethanol solution for 20 min for chemisorption of N3. Because TiO₂ has a wide band gap energy and low sensitivity in the wavelength of visible light, it requires a photosensitizer such as N3 to achieve photoconductivity in the visible range. N3 is known to effectively inject electrons into the conduction band of TiO₂, as it has a suitable electric potential and carries attachment sites, i.e., carboxyl acid groups, for chemisorption onto the surface of TiO₂.⁹

Figure 7 shows the typical response behaviors of the first-order diffracted beam intensities of PR-LC cells with photoconductive layers of (a) N3-chemisorbed TiO₂ (cell C), and (b) C₆₀-doped PVK/TiO₂ nanocomposite (cell A), with, respectively, dc fields of 1.7 V/μm and 3.2 V/μm applied at 0 s of time. In

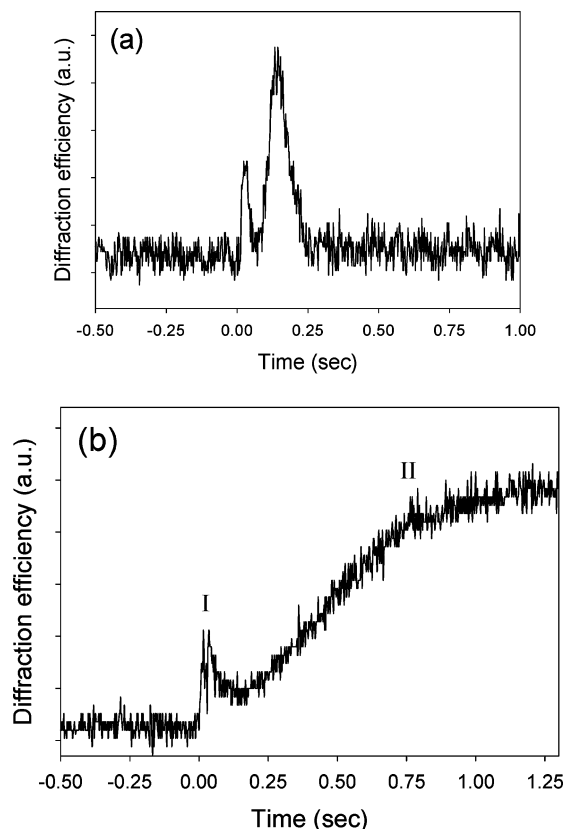


Figure 7. The typical response behaviors of the first-order diffracted beam intensities of PR-LC cells with photoconductive layers of (a) N3-chemisorbed TiO_2 (cell C), and (b) C_{60} -doped PVK/ TiO_2 nanocomposite (cell A). dc fields were applied to the LC cells at 0 s of time.

cell C, the diffraction efficiency revealed two discernible peaks, indicating temporary formation of a diffraction grating. When illuminated, N3, attached on the surface of TiO_2 , absorbs photons and becomes excited. Ruthenium of N3 generates electrons, and the electrons are transported to the N3– TiO_2 interface through a carboxylated bipyridyl ligand, an attachment group of N3, and injected into the conduction band of TiO_2 . In the TiO_2 layer, electrons diffuse out and induce space-charge field temporally.²³ Since there is no trap site in the TiO_2 layer, the induced space-charge field cannot be maintained, and photogenerated electrons drift to the electrode or the LC layer, along the direction of the external dc field. Due to the difference in the electron-drift condition of two TiO_2 layers, the diffraction efficiency shows two peaks.²³ In the PR-LC cell with one TiO_2 layer, only one diffraction efficiency peak was observed.²³

In cell A, the response behavior of the diffraction efficiency is divided into two regions, I and II. In region I, the diffracted beam intensity increased suddenly and decayed abruptly, showing two point peaks, which is equivalent in shape and generation time-scale to the behavior of cell C. In region II, the diffraction efficiency increased gradually, similar to a typical PR-LC cell (see Figure S3). The response behavior of region I reflects the unique characteristic of an inorganic layer without charge-trap sites, not observed in a PVK layer, and thus provides evidence that electrons were injected from C_{60} -doped PVK into TiO_2 before the space-charge field was generated in the PVK layers. Photoinduced charge transfer and recombination processes at the interface of organic conjugated polymer and inorganic TiO_2 are currently the subject of intense study.¹⁰ The results described above shows charge transport in a heterojunction of the polymer and TiO_2 by the electrooptic method.

Because a TiO_2 layer without a photosensitizer has low sensitivity in the visible range, the diffraction peaks of region I can be attributed to the space-charge field formed by electrons injected from the C_{60} -doped PVK layer. No beam diffraction was observed in the layer-structured PR-LC cell with pure mesoporous TiO_2 layers.

The response behaviors of cell C and region II of cell A show the characteristic of a photoconductive inorganic layer. They only differ in electron sources, directly attached N3 and C_{60} -doped PVK, respectively. Region II of cell A is the characteristic of a photoconductive polymer layer, which cannot be observed in cell C. The diffraction formation of region II can meanwhile be attributed to the space-charge field generated in the PVK layer after temporary generation of the space-charge field in the TiO_2 layer. Because the PVK layer has charge-trap sites, mobile charges, that is, holes in the PVK layer, are trapped, and the space-charge field is maintained. The diffraction efficiency of region II of cell A is greatly enhanced. The enhanced diffraction efficiency is caused by electron injection from the PVK layer into the TiO_2 layer. Limitation of charge-trap sites in the PVK layer could cause recombination of photogenerated charges and results in a decreased number of photogenerated charges. However, after electron injection into the TiO_2 layer, more free holes would remain without charge recombination and these could then participate in the generation of the space-charge field in PVK layers. In the nanocomposite layer, the mesoporous TiO_2 layer acted as a charge-recombination blocker by withdrawing electrons from the PVK. Therefore, it is concluded that the novel nanocomposite layer could enhance the photorefractive effect of the layer-structured PR-LC cell.

3. Conclusions

In summary, photoconductive layers of PR-LC cells were fabricated with PVK-infiltrated mesoporous TiO_2 films. The maximum of the first-order Raman–Nath diffraction efficiency in the layer-structured PR-LC cell with novel photoconductive layers was observed to be as high as 42.9%. The addition of a TiO_2 layer to the photoconductive layer increased the first-order Raman–Nath diffraction efficiency from 24% to 42.9%. This enhancement is attributed to enhanced local density of photogenerated positive charges arising from the rapid drain of electrons to the mesoporous TiO_2 layer. Electron injection from the PVK layer into the mesoporous TiO_2 layer would reduce the charge recombination in the PVK layer, and therefore a large number of holes in the PVK layer would participate in formation of the space-charge field.

4. Experimental Section

Well-organized mesoporous TiO_2 films were obtained as follows:¹² The sol was prepared with a molar ratio of 1 TiCl_4 (Aldrich, 99.9%):44.6 EtOH (Merck, 99.9%):0.0645 polyoxyethylene (20) cetyl ether (Brij 58, Aldrich). The prepared sol was evaporated at 40 °C in an oven within 1 h in order to remove HCl produced during reaction. Some ethanol was also evaporated (less than 5%), but the sol was not aged further. The sol was then deposited on ITO glass by spin coating, and the film was aged at 57% RH (relative humidity) for 1 h. Finally, the film was calcined at 150 °C for 2 h and at 300 °C for 4 h, raising the temperature at a rate of 2 °C/min.

The thickness of the prepared film was measured by a surface profiler system (α -step). TEM was performed on a Philips CM-200 microscope operating at 200 kV, and XPS depth profiling was performed on an ESCALAB 210.

Acknowledgment. This work was partially supported by the Center for Ultramicrochemical Process Systems, and the Nano R & D Program of the Korea Science and Engineering Foundation.

Supporting Information Available: The XPS depth profile of mesoporous TiO₂ thin film, diffraction efficiencies with various LC layer thicknesses, and response behavior of the diffracted beam intensity of a PR-LC cell with C₆₀-doped PVK layers. This material is available free of charge via the Internet at <http://pubs.acs.org>.

References and Notes

- (1) (a) *Photorefractive Materials and Their Applications I & II*; Günter, P., Huignard, J.-P., Eds.; Springer-Verlag: Berlin; 1988. (b) Giuliano, C. R. *Phys. Today* **1981**, April, 27.
- (2) Moerner, W. E.; Grunnet-Jepsen, A.; Thompson, C. L. *Annu. Rev. Mater. Sci.* **1997**, 27, 585.
- (3) Khoo, I. C.; Li, H.; Liang, Y. *Opt. Lett.* **1994**, 19, 1723.
- (4) Rudenko, E. V.; Sukhov, A. V. *JETP Lett.* **1994**, 59, 142.
- (5) Wiederrecht, G. P.; Yoon, B. A.; Wasielewski, M. R. *Science* **1995**, 270, 1794.
- (6) Golemme, A.; Volodin, B. L.; Kippelen, B.; Peyghambarian, N. *Opt. Lett.* **1997**, 22, 1226.
- (7) (a) Ono, H.; Kawatsuki, N. *Appl. Phys. Lett.* **1997**, 71, 1162. (b) Ono, H.; Kawatsuki, N. *Opt. Commun.* **1998**, 147, 237. (c) Mun, J.; Yoon, C. S.; Kim, H.-W.; Choi, S.-A.; Kim, J.-D. *Appl. Phys. Lett.* **2001**, 79, 1933. (d) Wiederrecht, G. P.; Yoon, B. A.; Svec, W. A.; Wasielewski, M. R. *J. Am. Chem. Soc.* **1997**, 119, 3358.
- (8) (a) Arango, A. C.; Carter, S. A.; Brock, P. J.; Appl. Phys. Lett. **1999**, 74, 1698. (b) Barth, S.; Bäessler, S.; Rost, H.; Hörhold, H. H. *Phys. Rev. B* **1997**, 56, 3844. (c) Moses, D.; Wang, J.; Yu, G.; Heeger, A. J. *Phys. Rev. Lett.* **1998**, 80, 2685.
- (9) (a) Nazeeruddin, M. K.; Kay, A.; Rodicio, I.; Humphry-Baker, R.; Muller, E.; Liska, P.; Vlachoroulos, N.; Grätzel, M. *J. Am. Chem. Soc.* **1993**, 115, 6382. (b) Bach, U.; Lupo, D.; Comte, P.; Moser, J. E.; Weissörtel, F.; Salbeck, J.; Spreitzer, H.; Grätzel, M. *Nature (London)* **1998**, 395, 583. (c) Grätzel, M. *Prog. Photovolt. Res. Appl.* **2000**, 8, 171.
- (10) (a) Salafsky, J. S. *Phys. Rev. B* **1999**, 59, 10885. (b) van Hal, P. A.; Christiaans, M. P. T.; Wienk, M. M.; Kroon, J. M.; Janssen, R. A. J. *J. Phys. Chem. B* **1999**, 103, 4352. (c) Breeze, A. J.; Schlesinger, Z.; Carter, S. A. *Phys. Rev. B* **2001**, 64, 125205. (d) Salafsky, J. S.; Lubberhuizen, W. H.; Schropp, R. E. I. *Chem. Phys. Lett.* **1998**, 290, 297.
- (11) (a) Kresge, C. T.; Leonowiz, M. E.; Roth, W. J.; Vartuli, J. C.; Beck, J. S. *Nature (London)* **1992**, 359, 710. (b) Yang, P.; Zhao, D.; Margolese, D. I.; Chmelka, B. F.; Stucky, G. D. *Nature (London)* **1998**, 396, 152. (c) Yang, P.; Zhao, D.; Margolese, D. I.; Chmelka, B. F.; Stucky, G. D. *Chem. Mater.* **1999**, 11, 1813. (d) Alberius, P. C. A.; Frindell, K. L.; Hayward, R. C.; Kramer, E. J.; Strucky, G. D.; Chmelka, B. *Chem. Mater.* **2002**, 14, 3284.
- (12) Jang, K.-S.; Song, M.-G.; Cho, S.-H.; Kim, J.-D. *Chem. Commun.* **2004**, 13, 1514.
- (13) Coakley, K. M.; Liu, Y.; McGehee, M. D.; Frindell, K. L.; Stucky, G. D. *Adv. Funct. Mater.* **2003**, 13, 301.
- (14) (a) Krishnamoorti, R.; Vaia, R. A.; Giannelis, E. P. *Chem. Mater.* **1996**, 8, 1728. (b) Vaia, R. A.; Giannelis, E. P. *Macromolecules* **1997**, 30, 8000.
- (15) Shanahan, M. E. R.; Carre, A. In *Nano-Surface Chemistry-Nanometric Solid Deformation of Soft Materials in Capillary Phenomena*; Marcel Dekker: New York; 2001.
- (16) (a) Kim, H.-W.; Jung, S.; Yoon, C. S.; Kim, J.-D. *Appl. Phys. B: Laser Opt.* **2002**, 75, 123. (b) Kim, H.-W.; Jung, S.; Yoon, C. S.; Kim, J.-D. *Appl. Phys. B: Laser Opt.* **2003**, 77, 427.
- (17) Yeh, P. In *Introduction to Photorefractive Nonlinear Optics*; Wiley: New York, 1993; p 118.
- (18) Ono, H.; Saito, I.; Kawatsuki, N. *Appl. Phys. B: Laser Opt.* **1998**, 66, 527.
- (19) (a) Khoo, I. C. *Phys. Rev. A* **1981**, 23, 2077. (b) Durbin, S. D.; Arakelian, S. M.; Shen, Y. R. *Phys. Rev. Lett.* **1981**, 47, 1411.
- (20) Eichler, H. J.; Günter, P.; Pohl, D. W. In *Laser-Induced Dynamic Gratings*; Tamir, T., Ed.; Springer: New York, 1986.
- (21) Bartkiewicz, S.; Matczyszyn, K.; Miniewicz, A.; Kajzar, F. *Opt. Commun.* **2001**, 187, 257.
- (22) (a) Coakley, K. M.; McGehee, M. D. *Appl. Phys. Lett.* **2003**, 83, 3380. (b) Savenije, T. J.; Warman, J. M.; Goossens, A. *Chem. Phys. Lett.* **1998**, 287, 148. (c) Pettersson, L.; Roman, L.; Inganas, O. *J. Appl. Phys.* **1999**, 86, 487.
- (23) Jang, K.-S.; Cho, S.-H.; Kim, J.-D. Unpublished.